J Mater Sci (2010) 45:4321–4331
DOI 10.1007/s10853-010-4418-3

EUROMAT 2009

Flux-assisted spreading of an Al–7 wt%Si alloy on TiC

V. H. López · A. R. Kennedy · R. García

Received: 22 October 2009 / Accepted: 13 March 2010 / Published online: 27 March 2010

Abstract The effect of a K–Al–F-based flux was investigated on the wettability of TiC by an Al–7 wt%Si alloy in the interval of temperatures between 660 and 900 °C in Ar and in atmospheric air. Null spreading was observed without flux whereas perfect wetting was enabled by the flux in both atmospheres. The liquid flux, which provides a locally protective atmosphere by spreading on the surfaces of the substrate and eventually on the Al alloy, dissolves the aluminium oxide covering the molten alloy enabling thus direct contact between the liquid alloy and the TiC substrate. The low tensions for the solid/flux and liquid metal/flux interfaces facilitate spontaneous spreading and instantaneous wetting. Meanwhile, the flux is displaced to the lateral periphery of the substrate and to the surface of the liquid. Under the resolution of the scanning electron microscope, microstructural examination of the interfaces did not reveal reaction products. Rapid infiltration of the alloy into TiC/flux compacts, at low temperatures, correlated well with the flux-assisted spreading kinetics observed.

Introduction

The processing route for manufacturing metal matrix composites reinforced with ceramic particles is dictated by the wettability of a given metal–ceramic system. Because this property describes the extent of intimate contact between a liquid and a solid, it is necessary to have a parameter to estimate it. The contact angle, θ, of a liquid on the solid surface is the parameter used to measure the degree of wetting by the sessile drop method. The lower the contact angle, the larger the affinity of the metal–ceramic system [1–3]. Although the sessile drop test is an oversimplification of true and complex phenomena occurring during fabrication of composites either by infiltration of porous ceramic bodies or incorporation of ceramic particles into melts, it is widely accepted and used as an index to define processing route and its parameters.

Wettability in Al–ceramic systems is governed in the first instance by the presence of an oxide layer that prevents molten Al from achieving intimate contact with the ceramic. This barrier is responsible for a non-wetting-to-wetting transition at temperatures above 900 °C. Attempts have been made to suppress the effect of the oxide in molten Al by forming the droplet in situ on the substrates by dispensing the droplet through a capillary [4–7]. The non-wetting-to-wetting transition in the Al/SiC system was found to occur at ~750 °C by ruling out this barrier, in comparison to 950 °C for a droplet covered by a film of oxide [4]. Another method to overcome the barrier effects of oxide films has been devised by using fluxes [8–10]. Fluoride salts, known as fluxing agents, have the capability to dissolve aluminium oxide. Rocher and co-workers [8, 9] observed spontaneous wetting of SiC and C fibre preforms by Al between 650 and 900 °C.

TiC is an attractive ceramic that has been successfully used to reinforce aluminium matrices by virtue of their good wettability [10–14]. According to the contact angle data available in the literature and the time and temperature dependence observed in the Al–TiC couple, it appears to

V. H. López (✉) · R. García
Instituto de Investigaciones Metalúrgicas, Universidad Michoacana de San Nicolás de Hidalgo, A.P. 888, C.P. 58 000 Morelia, Michoacán, México
e-mail: composito@yahoo.com

A. R. Kennedy
Advanced Materials Research Group, School of Mechanical, Materials and Manufacturing Engineering, University of Nottingham, Nottingham NG7 2RD, UK

act as a reactive system in which spreading is driven by the formation of an Al_4C_3 layer at the interface [11–16]. It has been suggested, however, that spontaneous and instantaneous wetting at low temperature may exist in this system if the oxide layer is removed [10]. The objective of this study is to unveil the wettability of molten Al–7 wt%Si with TiC by removing the oxide skin with a K–Al–F-based flux and to achieve a deeper understanding of the flux-assisted infiltration of molten Al–7 wt%Si into TiC beds.

Experimental

Materials

A K–Al–F-based flux (a mixture of $KAlF_4$ and $KAlF_6$ close to the eutectic composition in the $KF–AlF_3$ system) and an Al–7 wt%Si alloy were used to conduct wetting experiments. The alloy was made by melting pure Al and adding 99.99% pure Si. Chemical analyses are listed in Table 1. TiC substrates were prepared from HV 120 grade TiC powders (H.C. Starck, Germany), with a $D_{50} = 1.5$ μm. TiC compacts, uniaxially pressed, were sintered under flowing Ar in a tube furnace at 1550 °C for 5 h. The sintered density of the substrates was measured using the Archimedes method (ASTM 373-00), achieving 88 ± 1% with approximately 8.9% open porosity. This was the maximum density that could be achieved with this experimental set up. The sintered discs were ground and polished to a mirror-like finish with 1-μm diamond paste. Lattice parameters were determined in both the powder and the polished substrates using the Nelson–Riley function [17], using *d*-spacings obtained by X-ray diffraction (0.01°/s for 2θ angles from 20° to 140° with a dwell time of 3 s using Cu Kα radiation), and the values were determined to be 0.43267 and 0.43265 nm, respectively. This indicated that the sintering process did not affect the stoichiometry of the TiC which corresponds to a value close to unity, according to the variation in the lattice parameter with C/Ti ratio [18].

Wetting experiments

The sessile drop technique was used to conduct wetting experiments. The experimental set-up employed is essentially that used in reference [14] but without a high vacuum system. Experiments were performed with TiC substrates at 900 °C, without using flux, under a gentle flow of Ar (commercial purity). Experiments using flux were carried out between 660 and 900 °C under flowing Ar and in atmospheric air. Approximately 0.3 g of flux was deposited on the polished surface of the TiC substrates by using a methanol-based paint. The flux coating was allowed to dry naturally. Cubic pieces of Al–7 wt%Si weighing 0.8 ± 0.01 g were placed on the as-polished or flux-coated substrates. The sample holder with the assembly was positioned in the cold zone of the furnace. The system was closed and heated to the desired temperature under flowing Ar or air as required. Once the desired temperature had stabilised, the sample was gently transferred into the hot zone using a magnet. The progress of the sessile drop experiments was followed with a digital camera, either by taking photographs or video recording at 15 frames per second. In both cases, a 2× optical zoom was used. After completion of the experiments, the samples were removed from the hot zone to arrest any further interaction by inducing fast cooling.

The solidified drops on the TiC substrates were cut in half, mounted in conductive bakelite and metalographically prepared. Throughout the metallographic preparation, the use of water was avoided to preserve the presence of any Al_4C_3 that might be present. Instead, methylated spirit was used. The interfaces were examined using scanning electron microscopy (SEM) and energy dispersive X-ray (EDX) techniques.

Differential scanning calorimetry

In order to follow the sequence of events during the spreading experiments, differential scanning calorimetric (DSC) runs were carried out in atmospheric air, using a Netzsch 404 DSC. Samples were placed in BN crucibles and heated to 800 °C, at a heating rate of 20 °C/min. Al_2O_3 crucibles could not be used due to its interaction with the flux. BN crucibles did not show any 'noise' in the traces as a result of interaction with the flux or oxidation. Runs with the individual materials were conducted to detect the thermal events that take place in each material during heating. The combinations involved in the infiltration process were then evaluated, namely TiC/flux, flux/Al–7 wt%Si and TiC/flux/Al–7 wt%Si.

In situ observations of the infiltration kinetics

In order to gain insight into the relation between spreading and infiltration kinetics of molten Al and Al–7 wt%Si into TiC beds with the aid of a K–Al–F-based flux, the sessile drop apparatus was adapted and used to follow the evolution of infiltration using the experimental set-up shown in Fig. 1.

Table 1 Chemical composition of the Al and Al–7 wt%Si alloy used (wt%)

Ti	Fe	Si	Cu	Mn	Mg	Al
<0.01	0.05	<0.01	<0.01	<0.01	<0.01	Balance
<0.01	0.02	6.9	<0.01	<0.01	<0.01	Balance

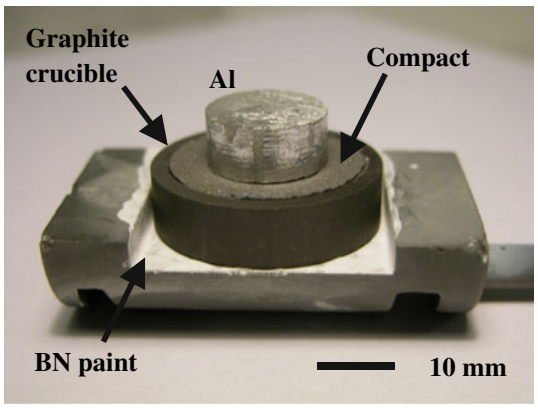

Fig. 1 Experimental set-up to follow the infiltration process

Experiments were performed under flowing Ar between 660 and 800 °C for Al and at 680 and 700 °C for Al–7 wt%Si. Approximately, 8.4 g of TiC/flux mixture in the mass ratio 3:1 was pressed in a 25-mm steel die to produce compacts, with an approximate porosity of 56%, which then were placed into the graphite crucibles. A piece of Al or Al–7 wt%Si weighing approximately 4 g was placed on the top surface of the compacts, which was calculated to be sufficient metal to fill the pores upon infiltration. The procedure followed was essentially that used in the sessile drop experiments. The progress of the experiments was recorded by taking photos with a digital camera. The infiltrated composites were removed from the crucibles, sand blast cleaned to remove the flux from the surface and metallographically prepared as described before.

Results

Wetting and spreading

A high contact angle was observed for the sessile drop experiment conducted without flux at 900 °C with no significant change after holding for 90 min. The presence of flux on the surface of the TiC substrates had a dramatic effect on spreading and wetting in both atmospheres. Melting of both the flux and the Al–7 wt%Si alloy, and full spreading of the molten alloy to a perfect wetting condition, took place in less than 2 min at 900 °C.

During the sessile drop experiments, a number of events were observed. Figure 2 shows the progress of the first stage of an experiment performed at 660 °C in air. The same behaviour was observed, during this stage, in all the experiments. The first photograph, 20 s after the assembly was positioned in the hot zone, shows the solid cube of metal resting on the also still solid flux. After approximately 3 min and 42 s, the flux starts to melt, 10 s later turns into fully liquid. The flux, upon melting, forms a liquid coating on the substrate and spreads on the still solid aluminium alloy. The liquid flux wets the alloy and the substrate, thus forming a 'bridge' between them along the basal periphery of the alloy, as indicated by the arrow in Fig. 2 (03:52). Both in Ar and in air, the flux was seen to interact with the surface of the metal, forming a darker layer along the basal periphery of the alloy, which eventually ascended its surface (photographs from 03:52 to 05:10), resulting in a shiny appearance to the metal (see photographs from 04:40 to 05:10). This process was seen to be stronger in air. When reaching approximately the mid-height of the alloy, as indicated by the arrow in Fig. 2 at 05:10 and after the piece of alloy had melted, the spreading process began for the high temperature experiments, whilst for those conducted at 750 °C and below, increasing periods of time elapsed before spreading took place.

Figure 3 shows the spreading at 660 °C in air. The spreading process is steady and smooth and this was characteristic over the whole interval of temperatures evaluated and independent of the atmosphere. In all the sessile drop experiments, the spreading process took place before the molten alloy adopted the typical spherical shape of a drop, as shown in Fig. 3. This fact, along with the presence of the flux forming a meniscus at the triple line, did not allow any measurement of the contact angle.

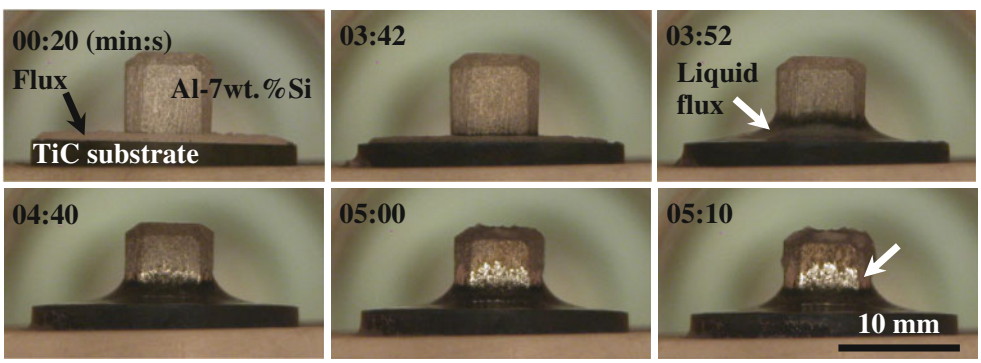

Fig. 2 Typical melting and spreading of the flux: experiment in air at 660 °C

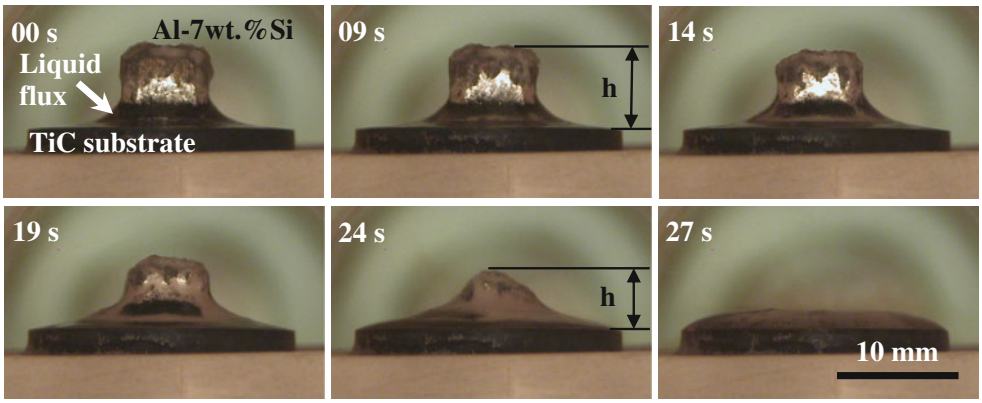

Fig. 3 Flux-assisted spreading of molten Al–7 wt%Si on TiC in air at 660 °C

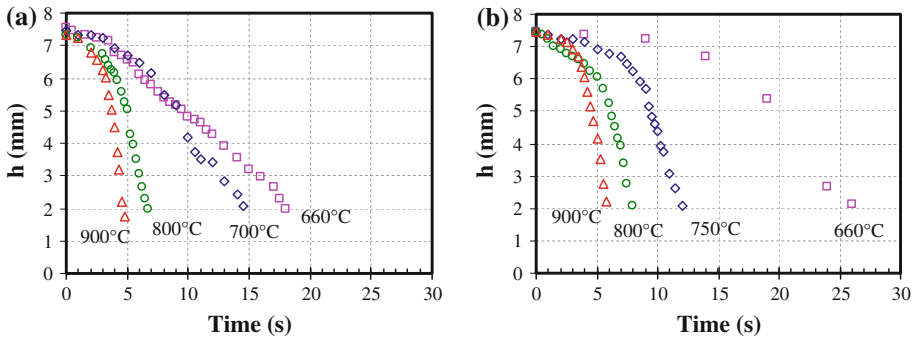

Fig. 4 Spreading kinetics of molten Al–7 wt%Si on TiC in **a** Ar and **b** air

Spreading kinetics

Owing to the steady spreading behaviour exhibited by the Al–7 wt%Si alloy over the entire temperature interval, it was possible to follow the spreading kinetics, as shown in Fig. 4, by measuring the height of the liquid during the spreading process as illustrated by two photographs in Fig. 3. Measurements were performed with software facilities after proper calibration was made. The spreading curves for height versus time are characterised by a slow parabolic initial stage which then turns into a linear stage where spreading is more rapid. From these plots, it is observed that the spreading rate is slightly faster in Ar than in air and that there is a temperature dependency on the spreading rate as it increases by at least three orders of magnitude from 660 to 900 °C.

A greater angularity to the shape of the aluminium alloy droplet was retained in the experiments performed in air. This fact, however, did not present any significant delay in the spreading process, as observed in Fig. 5, in which the plot shown summarises the temperature dependency observed in the flux-assisted spreading of molten Al–7 wt%Si on TiC in both Ar and air atmospheres. The data obtained in this study are also compared with that for pure Al [19]. The spreading time was estimated from the point at which the droplet was molten but still standing, until the moment at which the liquid formed a convex shape on the substrate as observed in the last

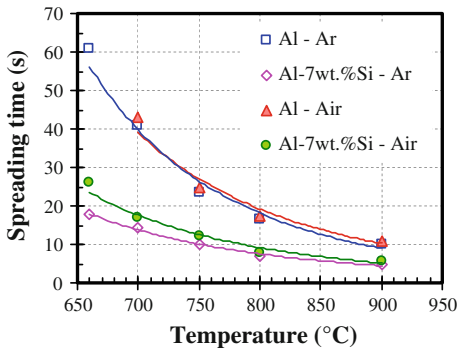

Fig. 5 Temperature dependency of the flux-assisted spreading of Al and Al–7 wt%Si on TiC

photograph in Fig. 3. The spreading time versus temperature curves show that the Al–7 wt%Si alloy spreads faster than pure Al and that the surrounding atmosphere does not play a significant role in the spreading time for a given temperature. During the experiments in air at low temperatures, an intermittent flame was observed in the meniscus formed between the liquid flux, the molten Al–7 wt%Si and the TiC substrate indicating combustion. Figure 6 shows the typical appearance of the assemblies after the wetting experiments. It can be observed that the flux is displaced from the Al–7 wt%/TiC interface to coat the surface of the aluminium. Removal of the flux reveals that the molten alloy spreads across the entire top surface of the substrate.

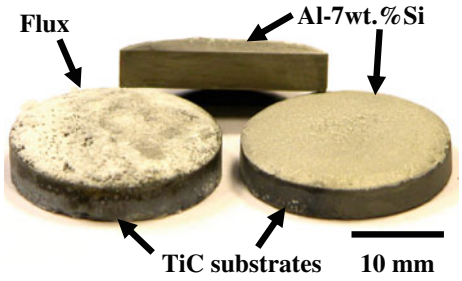

Fig. 6 Typical appearance of the substrate/droplet before (*left*) and after (*right*) removal of the flux

Interfacial characteristics

Figure 7 shows the microstructural features of the interfaces obtained after the wetting tests. At low and high magnifications, interfaces free of any visible reaction products were observed in both atmospheres and at all temperatures under the resolution of the SEM. Some degree of infiltration was found in the substrates as a result of the percentage of open porosity. Figure 8 shows an elemental X-ray dot map of an Al–7 wt%Si/TiC interface produced at 900 °C. It can be observed that eutectic silicon is segregated along the interface.

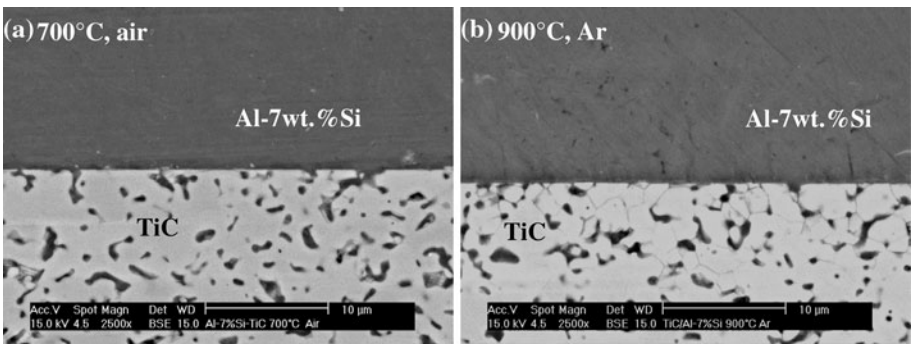

Fig. 7 Interfacial characteristics: at **a** low and **b** high temperature

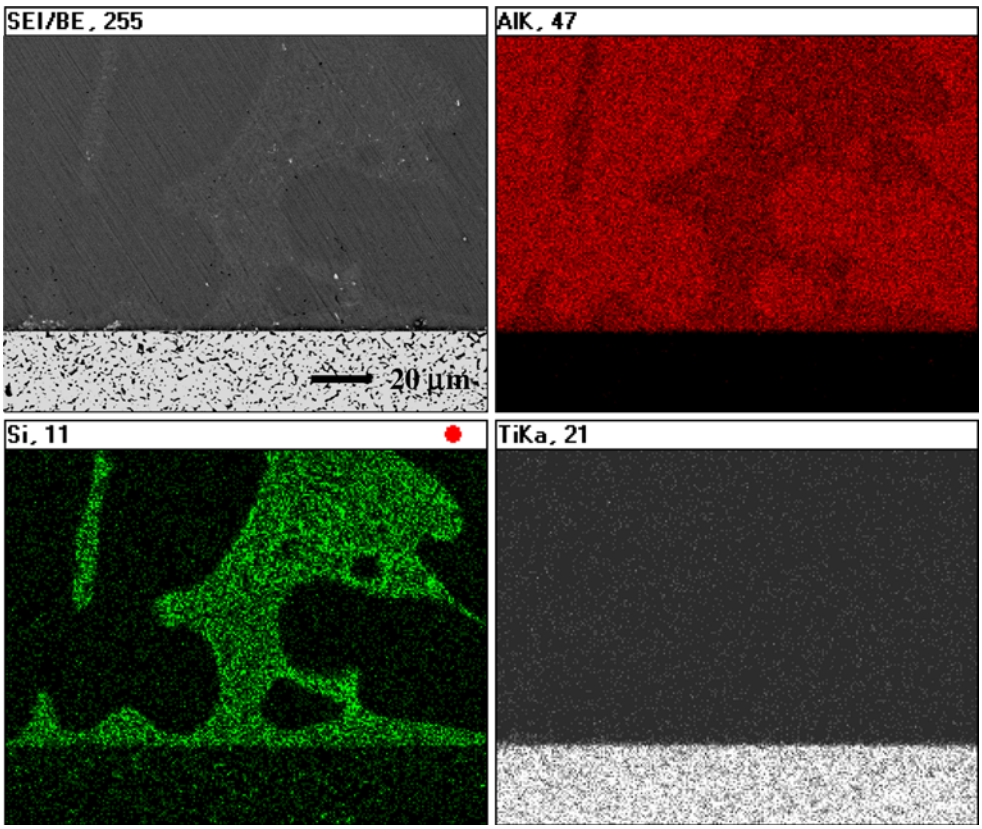

Fig. 8 Elemental X-ray dot map of the Al–7 wt%Si/TiC interface produced at 900 °C

Differential scanning calorimetry

Figure 9 shows the DSC traces for the single components (TiC, flux and the Al–7 wt%Si alloy) and for binary and ternary combinations of these phases when heating under atmospheric air. According to Fig. 9a, melting of the Al–7 wt%Si alloy exhibits two overlapping endothermic events, melting of the eutectic at 577 °C and melting of primary aluminium at approximately 603 °C. The Al–Si alloy is fully molten at 613 °C. Although an endotherm can be observed in the trace for the flux at low temperature, followed by two minor events, these events correspond to the release of moisture from the flux and a number of solid-state phase transformations. Melting of the flux occurs at approximately 545 °C. Exothermic oxidation of TiC occurs in air in a number of stages, starting at approximately 430 °C.

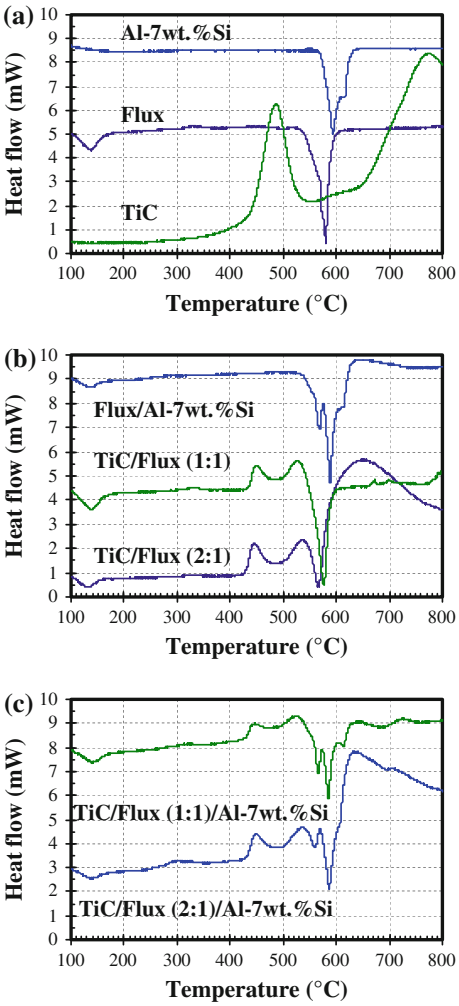

Fig. 9 DSC traces in air for the single components and combinations of the phases involved in the flux-assisted spreading process. The *numbers between parentheses* indicate the mass ration between TiC and flux

Figure 9b shows the thermal events for the different binary combinations of TiC, flux and the Al–7 wt%Si alloy. Flux was present in all the samples, and it was observed to melt at the same temperature in all the cases, at 545 °C. This melting event is overlapping with the Al–Si melting, and after melting of the alloy is completed, there is an exothermic event followed by the trace returning to the baseline. The TiC/flux couples exhibit two consecutive exothermic events, starting at approximately 430 °C, followed by endothermic melting of the flux. For the 1:1 mass ratio, after flux melting, the trace returns to the baseline, whereas for the 2:1 mass ratio, an exothermic event is observed.

Figure 9c shows the thermograms for the ternary mixtures. In all the samples, TiC and flux are present; accordingly, there are two consecutive exothermic events followed by endothermic melting of the flux and the alloy. In the TiC/flux/Al–7 wt%Si system for a ratio 2:1, after melting of the alloy, the trace describes a large exothermic event which is interrupted by another small thermal event; after this, the trace seems to head back to the baseline. For the same combination, but for a ratio 1:1, the large exotherm, observed for the 2:1 ratio after melting of the flux, does not take place.

In situ observations of the infiltration kinetics

The fast rate of infiltration prevented any recording of the events in the majority of the experiments. It was possible, however, to follow in detail the process at 660 °C for Al in Ar, as shown in Fig. 10. The photographic sequence shows the assembly from the point at which it was positioned in the hot zone of the furnace. Melting of the Al piece took a long time, as the overheating is only about 10 °C, and after 50 min the Al becomes liquid and gets encapsulated within a shell of aluminium oxide. Three minutes later, the onset of a cleaning action was observed, as indicated by the arrows in Fig. 10.

After complete cleaning of the droplet (photograph at 58 min), the initial arrangement resembles that for the sessile drop experiments, and simultaneous spreading and infiltration take place. It can be seen that the viscous Al has a tendency to spread over the top surface of the compact and then to decrease its height and almost disappear as the liquid infiltrates the compact. Infiltration took place at 660 °C approximately 7 min after the point at which the aluminium oxide started to dissolve, but in about 2 min from the point at which cleaning was complete.

Observations indicate that the infiltration process occurs in the same way at higher temperatures but much more rapidly as the overheating of the melt is increased. This assumption is confirmed as shown in Fig. 11 in which the infiltration was observed at 750 °C. In this instance, the infiltration occurred 8.5 min after the assembly was placed

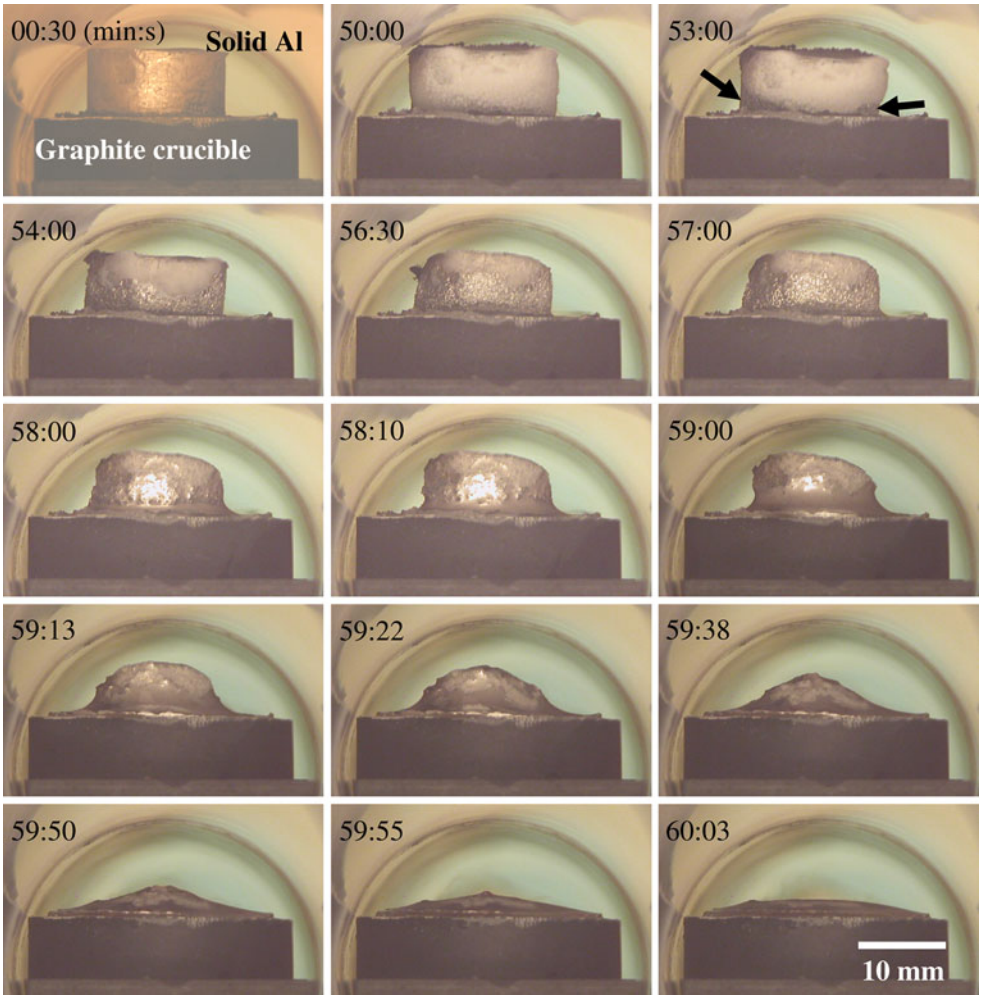

Fig. 10 Detailed evolution of the flux-assisted infiltration of Al into a TiC compact at 660 °C in Ar (TiC/flux mass ratio 3:1)

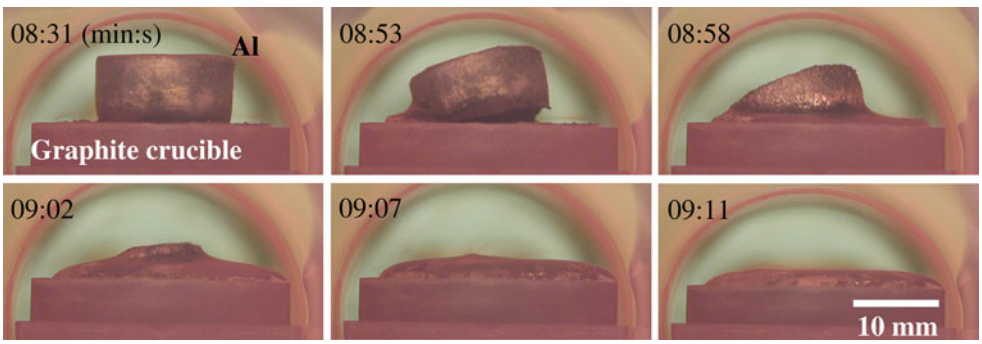

Fig. 11 Evolution of the flux-assisted infiltration of Al into a TiC compact at 750 °C in Ar (TiC/flux mass ratio 3:1)

in the hot zone. As observed in the sessile drop experiments for Al [19], the angular block of Al tipped over before spreading over the top surface of the compact as a result of the onset of infiltration. The entire infiltration process occurred in no more than 20 s. Infiltration of the Al–7 wt%Si alloy, was, generally speaking, seen to be faster than that for Al with the result it was even more difficult to capture details of the process. Nevertheless, Fig. 12 shows the evolution of infiltration of the alloy at 680 °C in Ar and provides a good description of the process. During heating, the still solid alloy turned very dark, a sign of the effect of Si on the oxidation and composition of the oxide film, and when melted, it adopted the shape of a spherical drop as a result of its significantly larger mass, in comparison to the

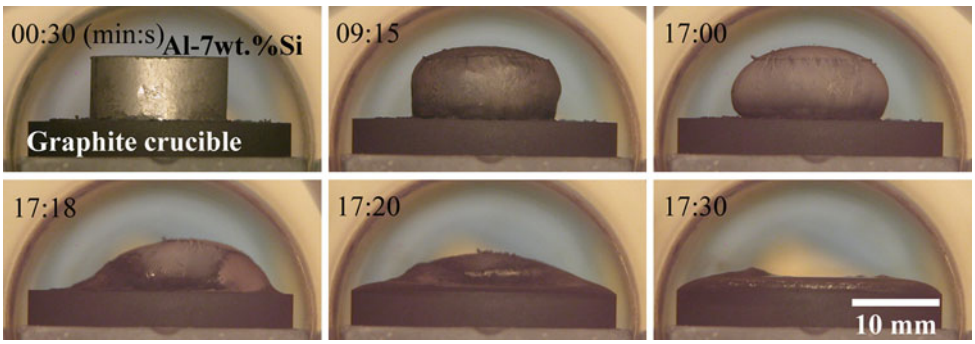

Fig. 12 Evolution of the flux-assisted infiltration of Al–7 wt%Si into a TiC compact at 680 °C in Ar (TiC/flux mass ratio 3:1)

mass used for the sessile drop experiments, its lower melting point, surface tension and viscosity compared to pure Al. In this case, the liquid also spreads on the top of the surface of the compact whilst infiltrating into it. Infiltration took less than 30 s.

Figure 13 shows the infiltrated samples after the experiments along with typical microstructures. In Fig. 13a, it can be clearly appreciated that the flux was expelled from the compact when it was infiltrated. Metallographic examination of the infiltrated samples revealed the presence of flux trapped within the Al matrix, with the Al–7 wt%Si–TiC sample exhibiting these defects to a larger extent. The Al–TiC sample was found to be free of any reaction products, whilst the Al–7 wt% sample exhibited the presence of small blocky and needle-shaped intermetallics, such as those indicated by the arrows in Fig. 13c, and according to EDX analysis with the approximate chemical composition $TiAl_{2.43}Si_{0.38}$. In the same micrograph, small black features are also observed, which correspond, however, to microporosity within the matrix, and in this case are associated with the trapped flux.

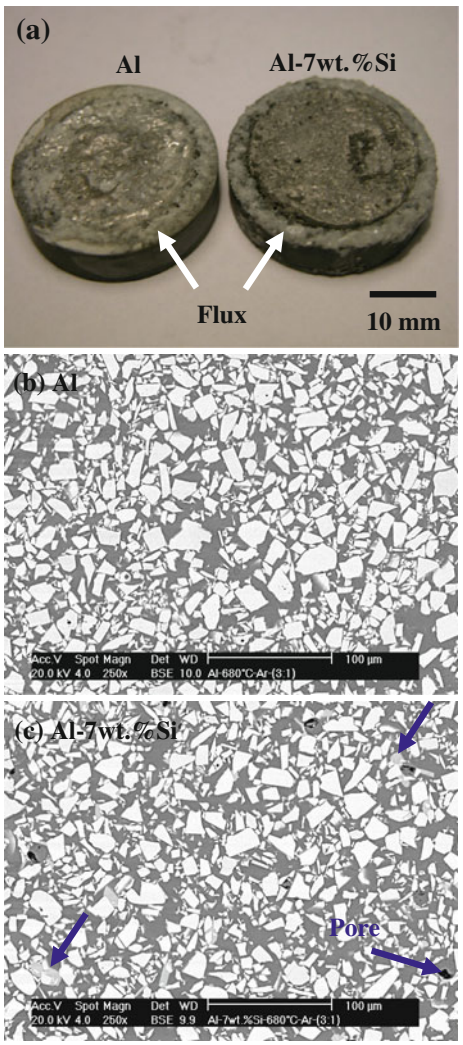

Fig. 13 Typical appearance of the infiltrated composites within the graphite crucible and microstructures of TiC/flux compacts (mass ratio 3:1) infiltrated at 680 °C in Ar

Discussion

Wetting and spreading

For Al and Al-alloys to spread on and wet TiC, the oxide skin has first to be removed, and it occurs when the partial pressure of Al_2O is low enough, at a given temperature above 800 °C (for example, 8×10^{-5} Pa at 900 °C), so that deoxidation of the droplet takes place according to reaction (1) [4–7, 13, 16]. This condition is only achieved in high vacuum systems. For this reason, it is evident that spreading of molten Al or any Al-alloy on TiC substrates is impossible, in air and even in Ar when oxygen is present as was observed at 900 °C in Ar in this study.

$$4Al(l) + Al_2O_3(s) = 3Al_2O(g) \quad (1)$$

The marginal difference in spreading times observed between atmospheres indicates that the use of a flux makes the surrounding atmosphere a non-critical issue. When the

flux melts, it spreads over the substrate and the solid Al-alloy, creating a local atmosphere that prevents oxygen contamination at the liquid metal/solid interface. Furthermore, the flux dissolves and weakens the oxide skin on Al, exposing clean and shiny surfaces as this process evolves and perhaps creating some local heating, through Al–flux–air interactions, that can give rise to the combustion flame observed during the sessile drop experiments at 660 °C in air. Schamm et al. [9] estimated a local temperature rise of about 150 °C due to the formation of Al_3Zr intermetallics during the spreading of molten Al on C and SiC with the aid of a K_2ZrF_6 flux. According to these authors, this exothermic effect significantly contributes to the degree of wetting achieved. A similar effect is not likely to take place in the spreading of Al–7 wt%Si on TiC assisted by a K–Al–F-based flux, since it contains only minor levels of Ti (0.062 wt%) and B (0.019 wt%) as impurities.

Dissolution of Al_2O_3 by cryolite melts, which is not that dissimilar to the flux used here, is a complex process which depends on a number of aspects. Whilst the dissolution process is not that well understood, it is, however, recognised that the process involves the endothermic reaction of the breaking of strong Al–O bonds by forming oxyfluoraluminate complexes with the fluoroaluminate species contained in the flux [20–23]. It is beyond the scope of this study to elucidate further about such mechanisms.

Nevertheless, when the flux dissolves the aluminium oxide layer, a solid TiC/liquid Al-alloy/liquid flux triple line is formed. This assumes that the flux underneath the Al-alloy is withdrawn which is likely to be the case as no traces of K or F were found at the TiC/solid Al–7 wt%Si interfaces using the SEM–EDX system. For the liquid flux to wet the liquid Al-alloy, the interfacial tension $\gamma_{Al/flux}$ has to be very low, and entrapment of the flux within the Al–7 wt%Si matrix during flux-assisted infiltration of TiC beds by Al–7 wt%Si indicates this to be the case [24, 25], and for the liquid Al-alloy to displace the TiC/flux interface and therefore spread, $\gamma_{TiC/Al} < \gamma_{TiC/flux}$. Because full spreading to a perfect wetting condition was observed from 660 to 900 °C, in both Ar and air, it is obvious that the latter condition is met, meaning that $\gamma_{TiC/Al} < \gamma_{TiC/flux} < \gamma_{TiC/gas}$. Thus, the replacement of the solid/gas and liquid metal/gas interfacial tensions with solid/flux and liquid metal/flux interfaces with lower forces, enables spreading and wetting of liquid Al–7 wt%Si on TiC to take place spontaneously and instantaneously.

The stages and mechanism by which TiC oxidises have been studied [26]. The DSC trace for the TiC agrees well with these studies. By virtue of the marginal difference between spreading times in Ar and in air, it is clear that the flux must play an important role in this regard. Heating in the sessile drop rig is faster than the heating rate used in the DSC. Thus, a kinetic effect shifts the onset of oxidation of the TiC to higher temperatures, but still some oxidation must occur before melting of the flux arrests further oxidation. In this context, the K–Al–F-based flux is capable of dissolving light oxidation products such as oxycarbides, suboxides and anatase formed on the surface of the TiC substrate, so that the mechanism of spreading discussed above is enabled.

Spreading kinetics

In comparison with pure Al, the Si-containing Al alloy was found to spread faster. It is well known that Si decreases the surface tension and viscosity of Al. Consequently, it acts as a surfactant in that, by being adsorbed at the liquid surface and segregating to the Al/TiC interface, it accelerates the spreading of Al on TiC, as observed in the sessile drop experiments. The surface tension and viscosity of aluminium and some aluminium alloys exhibit a linear temperature dependency and an Arrhenius-type behaviour [27, 28], respectively, such as

$$\gamma_T = \gamma_m - \frac{d\gamma}{dT}(T - T_m) \quad (2)$$

$$\eta_T = \eta_0 \exp\left(\frac{-E_a}{RT}\right) \quad (3)$$

where γ_T and η_T are the surface tension and viscosity, respectively, at temperature T, γ_m is the surface tension at the melting point, T_m, $d\gamma/dT$ is the surface tension coefficient and η_0 is a pre-exponential constant, whereas E_a is the apparent activation energy for viscous flow. Figure 14 plots the variation in the surface tension and viscosity in the interval of temperature employed in the sessile drop experiments, for Al [28, 29], a binary Al–8 wt%Si alloy [30] and an A356 alloy (6.9 wt%Si, 0.34 wt%Mg) [29]. It is evident that the presence of silicon in aluminium decreases both the surface tension and viscosity. The lower surface tension coefficient, $d\gamma/dT$, for the alloy indicates that this alloy is less sensitive to changes in surface tension with temperature. These observations account for the

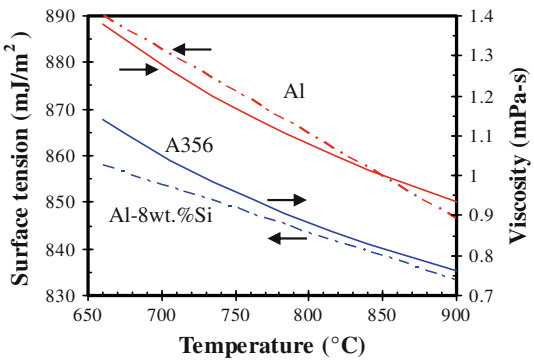

Fig. 14 Temperature dependency of the surface tension and viscosity for Al and Al–Si alloys [31, 34, 35]

different temperature dependency observed in the spreading time for Al and Al–7 wt%Si and for the shorter spreading times in the alloy.

Under the effect of a flux as wetting agent and in agreement with this study, the degree of wetting of molten Al on C and SiC was weakly temperature dependent [9]. The spreading times for the flux-assisted wetting, less than 1 min, are much shorter compared to 1 h for reactive wetting observed in the Al–TiC system [14] but very similar to the K_2ZrF_6 flux-assisted spreading of liquid Al on C and SiC [8, 9]. A wetting dynamics like that observed in the sessile drop experiments is not likely to have been slowed down or enhanced by the residual porosity in the substrates.

Interfacial microstructure

Time- and temperature-dependent spreading and wetting of molten Al and Al-alloys on TiC have been observed by many researchers under vacuum and in Ar (under a very low oxygen partial pressure) at temperatures between 750 and 1100 °C. In all cases, this was accompanied by reaction, either by the formation of an Al_4C_3 reaction layer at the interface for stoichiometric TiC, or the precipitation of $TiAl_3$ within the Al for hypostoichiometric $TiC_{(1-x)}$ [11–14]. Besides, reduction in the C/Ti ratio enhanced wetting at lower temperatures and accelerated spreading kinetics due to the increased metallic character in the $TiC_{(1-x)}$ bonds [12]. Also, it is known that dissolution of TiC in molten Al is rather slow [31], whereas the presence of silicon in aluminium significantly enhances the kinetics of the reaction [32]. Furthermore, it is established that the mechanism of dissolution is different at lower temperatures than at higher, TiC being partially stable in the latter case [31–34]. In the flux-assisted sessile drop experiments, molten Al–7 wt%Si was in contact with TiC for less than 1 min during experiments conducted at 900 °C, whereas at 660 °C, the longest contact time between the liquid metal and the TiC substrates was estimated to be no more than 3 min. The resulting Al–7 wt%Si/TiC interfaces were found to be, under the limits of resolution of the SEM, free from any reaction products over the whole interval of temperatures studied. This fact indicates that a genuine affinity exists in terms of wettability and adhesion, at low temperatures, if the Al_2O_3 is efficiently removed. Thus, if spreading of Al melts on TiC is driven by a chemical reaction, it must occur at a nanointerfacial level. Further characterisation by transmission electron microscopy of the interfaces would be required to clarify this issue.

In situ observations of the infiltration kinetics

Typically, capillary infiltration of molten Al into TiC preforms under Ar at temperatures higher than 860 °C exhibits parabolic-type profiles, preceded by an incubation period which is temperature dependent. This event is associated with the unstable contact angle observed in wetting experiments [11, 13] which is primarily linked to the deoxidation of the Al drop according to reaction (1).

In the flux-assisted infiltration process, a temperature-dependant period of time prior to infiltration was also observed and, in this instance, it can be related to the time required for the flux to dissolve the aluminium oxide. As observed in the sessile drop experiments and reflected in the parabolic portion and spreading rate of the spreading curves, this stage occurs more rapidly at higher temperatures. This may in part be due to the shorter period of time for the Al to melt as a result of higher heating rates, since it was obvious that there was a more noticeable interaction between the flux and the Al when the latter becomes liquid. As commonly occurs in metal/ceramic systems, infiltration was more rapid at higher temperatures and faster for Al–7 wt%Si than for Al. Because the spreading behaviour observed suggests an instantaneous perfect wetting condition, i.e. $\theta = 0$, facilitated by the flux at any temperature, it is clear that a capillary pressure, i.e. $P_c < 0$, will be developed. The application of a K_2ZrF_6 coating to SiC particles has been observed to significantly decrease the threshold pressure for infiltration of molten Al or Al–12 wt%Si, but never achieving a negative pressure even with increasing flux content [35, 36]. An important aspect to consider is that although a capillary pressure is developed, it might not be enough to surpass gravity forces if the size of the porous channels is larger than certain critical value. The rate of infiltration is thus highly dependent on the morphology of the porous network of the bed and on the physical properties of the melts, i.e. surface tension and viscosity [11].

Conclusions

The effect of a K–Al–F-based flux has been investigated on the wettability and spreading behaviour of Al–7 wt%Si on TiC in the interval of temperatures between 660 and 900 °C in Ar and in air. Obtuse contact angles were observed between molten Al–7 wt%Si on TiC without flux and under Ar. In contrast, spreading to a perfect wetting condition was observed in less than 60 s, and before any drop with a spherical shape was formed when the flux was present. This occurred over the whole interval of temperatures evaluated, under Ar and in Air.

It was observed that as soon as the flux melts, it spreads over the TiC surface and also on the solid surface of Al-alloy, forming a concave meniscus between them along the basal periphery of the Al-alloy. As the temperature of the assembly increases further, interactions on the surface of

Al-alloy are enhanced, as a result of dissolution of the aluminium oxide covering the Al-alloy by the flux. The liquid flux provides a local atmosphere that prevents any oxygen contamination by isolating the surfaces from the surrounding atmosphere. When the alloy melts and the oxide layer has been weakened and dissolved by the flux, intimate contact occurs between the liquid and the TiC substrate. The low tensions for the solid/flux and liquid metal/flux interfaces facilitate spontaneous spreading and instantaneous wetting of liquid Al–7 wt% on the TiC substrates. Meanwhile, the flux is displaced to the lateral periphery of the substrate and to the surface of the liquid.

Although the spreading process was extremely rapid, it was found to be temperature dependent, the atmosphere having a weak effect in spreading kinetics. The Al–7 wt%Si alloy spreads more rapidly than pure Al due to its physical properties in molten state. According to the spreading behaviour observed, flux-assisted infiltration of Al melts into TiC/flux compacts occurs rapidly at low temperatures.

References

1. Savov L, Heller HP, Janke D (1997) Metallurgica 51:475
2. Delannay F, Froyen L, Deruyttere A (1987) J Mater Sci 22:1. doi:10.1007/BF01160545
3. Mortensen A, Jin I (1992) Int Mater Rev 37:101
4. Laurent V, Chatain D, Eustathopoulos N (1987) J Mater Sci 22:244. doi:10.1007/BF01160579
5. Laurent V, Chatain D, Chatillon C, Eustathopoulos N (1988) Acta Metall 36:1797
6. Fuji H, Nakae H, Okada K (1993) Acta Metall Mater 41:2963
7. Ho HN, Wu ST (1998) Mater Sci Eng A 248:120
8. Rocher JP, Quenisset JM, Naslain R (1989) J Mater Sci 24:2697. doi:10.1007/BF02385613
9. Schamm S, Fedou R, Rocher JP, Quenisset JM, Naslain R (1991) Metall Trans A 22:2133
10. Kennedy AR, Karantzalis AE (1999) Mater Sci Eng A 264:122
11. Muscat D, Drew RAL (1994) Metall Mater Trans A 25:2357
12. Frumin N, Frage N, Polak M, Dariel MP (1997) Scr Mater 37:1263
13. Contreras A, López VH, León CA, Drew RAL, Bedolla E (2001) Adv Technol Mater Mater Proc J 3:27
14. Leon CA, Lopez VH, Bedolla E, Drew RAL (2002) J Mater Sci 37:3509. doi:10.1023/A:1016523408906
15. Contreras A, Bedolla E, Perez R (2004) Acta Mater 52:985
16. Froumin N, Frage N, Polak M, Dariel MP (2000) Acta Mater 48:1435
17. Cullity BD (2001) Elements of X-ray diffraction. Prentice Hall, New York
18. Storms EK (1967) The refractory carbides. Academic Press, New York, pp 1–17
19. Lopez VH, Kennedy AR (2006) J Colloid Interface Sci 298:356
20. Haverkamp RG, Welch BJ (1998) Chem Eng Proc 37:177
21. Lubyova Z, Danek V (1995) Chem Pap 49:59
22. Gerlach J, Henning U, Kern K (1975) Metall Trans B 6:83
23. Danek V, Gustavsen OT, Ostvold T (2000) Can Metall Q 39:153
24. Lee MS, Terry BS, Grieveson P (1993) Metall Trans B 24:955
25. Lopez VH, Kennedy AR, García R (2009) Rev Latinoam Met Mater 29:49–58
26. Shimada S (1996) J Mater Sci 31:673. doi:10.1007/BF00367884
27. Brandes EA, Brook GB (1992) Smithells metals reference book. Butterworth-Heinemann, Oxford
28. Keene BJ (1993) Int Mater Rev 38:157
29. Wang D, Overfelt RA (2002) Int J Thermophys 23:1063
30. Goicoechea J, Garcia-Cordovilla C, Louis E, Pamies A (1992) J Mater Sci 27:5247. doi:10.1007/BF02403824
31. López VH, Kennedy AR, Lemus J (2010) Kovove Mater 48:17
32. Lopez VH, Scoles A, Kennedy AR (2003) Mater Sci Eng A 356:316
33. Frage N, Frumin N, Levin L, Polak M, Dariel MP (1998) Metall Mater Trans A 29:1341
34. Viala JC, Vincent C, Vincent H, Bouix J (1990) Mater Res Bull 25:457
35. Alonso A, Narciso J, Pamies A, Garcia-Cordovilla C, Louis E (1993) Scr Metall Mater 29:1559
36. Rodriguez-Guerrero A, Sánchez SA, Narciso J, Louis E, Rodriguez-Reinoso F (2006) Acta Mater 54:1821